

Phase evolution of layered cobalt oxides versus varying corrugation of the cobalt-oxygen basal plane

Hua Wu ^a

Max-Planck-Institut für Physik komplexer Systeme, Nöthnitzer Str. 38, 01187 Dresden, Germany

Received 28 July 2002 / Received in final form 10 October 2002

Published online 31 December 2002 – © EDP Sciences, Società Italiana di Fisica, Springer-Verlag 2002

Abstract. A general spin-state model and a qualitative physical picture have been proposed for a class of lately synthesized layered cobalt oxides (LCOs) by means of density functional calculations. As the plane corrugation of the cobalt-oxygen layer decreases, the LCOs evolve from a high-spin (HS) superexchange-coupled antiferromagnetic (AFM) insulator to an almost-HS AFM/ferromagnetic (FM) competing system where the FM coupling is mediated *via* the *p-d* exchange by an increasing amount of delocalized *pdσ* holes having mainly the planar O 2*p* character. It is tentatively suggested that the delocalized holes more than 0.3 per CoO₂ basal square are likely necessary for the insulator-metal and/or AFM-FM transitions in the corrugation-weakened LCOs. A phase control may be realized in LCOs by varying the plane corrugation (thus modifying the hole concentration) through an ionic-size change of the neighboring layers on both sides of the cobalt-oxygen layer. In addition, a few experiments are suggested for a check of the present model and picture.

PACS. 71.27.+a Strongly correlated electron systems; heavy fermions – 71.20.-b Electron density of states and band structure of crystalline solids – 75.10.-b General theory and models of magnetic ordering

1 Introduction

The phase diagrams of transition-metal oxides (TMOs) concerning their crystal structures, electronic/magnetic and transport properties drew very extensive attention in past decades, especially after the discoveries of the high-temperature superconducting cuprates and the colossal magnetoresistance (CMR) manganites. A great number of experimental and theoretical studies have exploited rich physics [1], which not only leads one to understanding (although incomplete so far) of the nature and origin of their fascinating properties but also provides a guide in search of novel function materials. As members of the 3*d* TMOs, the cobalt oxides are of current considerable interest. This is, on one hand, due to their potential technological utilities such as the analogs of the CMR perovskite manganite [2] $R_{1-x}A_x\text{MnO}_3$ (R = rare earth; A = alkaline earth)— $R_{1-x}A_x\text{CoO}_3$ [3] and $RBa\text{Co}_2\text{O}_{5+x}$ [4], and the lately synthesized layered cobalt oxides (LCOs, analogs of the superconducting cuprates) having a rich variety of phases although no superconductivity observed in them up to now — $\text{Sr}_{n+1}\text{Co}_n\text{O}_{2n+1}\text{Cl}_n$ (SCOC) are

insulating with decreasing resistivity as the number of CoO₂ layers increases [5]; $\text{Sr}_2\text{Y}_{0.8}\text{Ca}_{0.2}\text{Co}_2\text{O}_6$ is an AFM insulator [6,7] while $\text{Sr}_2\text{Y}_{0.5}\text{Ca}_{0.5}\text{Co}_2\text{O}_7$ is a magnetically glassy semiconductor and exhibits a pronounced FM interaction [6,8]; $\text{Bi}_2\text{A}_3\text{Co}_2\text{O}_{8+x}$ (A = Ca, Sr) are semiconducting while the Ba analog has a metal to semiconductor transition [9]. On the other hand, this is in fundamental viewpoints mainly because of an intriguing but (in many cases) controversial issue [10–18] on the Co spin state which plays a vital role in the physical properties of cobalt oxides. The Co spin state relies primarily on a competition between the crystal field (CF) and Hund exchange coupling [17,18], and it is also affected by a *pd* covalent effect [10–12], as well as external factors, *e.g.*, varying temperature induces a complex spin state transition as observed in LaCoO_3 [11]. In addition, a few relevant issues concentrate on their electronic/magnetic structures and the closely related transport behaviors.

In this paper, by means of density functional theory (DFT) [19] calculations, both a general spin-state model and a qualitative physical picture have been set up for LCOs which have a common structural feature—a plane corrugation of the cobalt-oxygen layer. The DFT calculations show at least a tendency that as the plane corrugation decreases, the cobalt evolves from a high-spin

^a Present address: Fritz-Haber-Institut der Max-Planck-Gesellschaft, Faradayweg 4-6, 14195 Berlin, Germany
e-mail: wu@fhi-berlin.mpg.de

(HS) state to an almost HS state with an increasing amount of delocalized $pd\sigma$ holes having mainly the planar O $2p$ character. The former is responsible for a superexchange (SE) [20] coupled AFM insulating nature, while the latter gives rise to a coexistence of (and a competition between) the inherent AFM insulating behavior and the hole-mediated $p-d$ exchange [21] FM metallicity. This picture, although seeming qualitative, consistently accounts for the rich and varying phases of LCOs as seen below, and it leads to a suggestion of a possible phase control mechanism in LCOs.

2 Computational details

The above LCOs [5–9] each contain a basic structure block, that is the deformed CoO_5 pyramid where the Co ion moves out of the O_4 basal square and into the pyramid. The ab -planar CoO_2 layer is formed by those corner-shared CoO_4 “squares” extended along the a and b axes. Thus a common plane corrugation actually exists in the so-called CoO_2 layer. A parameter D is defined here for a description of the plane corrugation, and it represents an average distance between the Co ion and the O_4 basal “square”.

The DFT calculations have been performed for the monolayered (1L) $\text{Sr}_2\text{CoO}_3\text{Cl}$ and for the bilayered (2L) $\text{Sr}_3\text{Co}_2\text{O}_5\text{Cl}_2$ and $\text{Sr}_2\text{Y}_{0.8}\text{Ca}_{0.2}\text{Co}_2\text{O}_6$, since their structure data are available among the above LCOs [5,7]. $\text{Sr}_2\text{CoO}_3\text{Cl}$ takes a tetragonal structure ($a = 3.9026 \text{ \AA}$, $c = 14.3089 \text{ \AA}$) at room-temperature (RT), and so does $\text{Sr}_3\text{Co}_2\text{O}_5\text{Cl}_2$ ($a = 3.9142 \text{ \AA}$, $c = 24.0098 \text{ \AA}$), while $\text{Sr}_2\text{Y}_{0.8}\text{Ca}_{0.2}\text{Co}_2\text{O}_6$ takes an orthorhombic structure ($a = 3.8291 \text{ \AA}$, $b = 3.8238 \text{ \AA}$, $c = 19.5585 \text{ \AA}$) at 260 K. Their D parameters are 0.325, 0.285, and 0.44 \AA , respectively.

Adopted in the DFT calculations is the full-potential linearly combined atomic orbitals band method [22], where no shape approximation is made for charge densities and potentials. A full-potential method should be preferable for descriptions of the lattice-distorted materials, compared with an atomic-spherical approximation. Sr $4p4d5s$, Co $3d4s$, O $2s2p$, and Cl $3s3p$ orbitals are treated as valence states. A virtual-crystal approximation is made for $\text{Sr}_2\text{Y}_{0.8}\text{Ca}_{0.2}\text{Co}_2\text{O}_6$, where a virtual atom with nuclear charge $Z = 0.8 \times Z_Y + 0.2 \times Z_{Sr} = 38.8$ takes the place of the $\text{Y}_{0.8}\text{Ca}_{0.2}$ site. This virtual-crystal approximation is acceptable, since in most cases the Y [Ca(Sr)] atom merely donates its $4d^15s^2$ [$4s^2(5s^2)$] valence electrons and scarcely contributes to the usually concerned valence bands around Fermi level (E_F). Thus, the virtual atom takes the formal +2.8 valence ($4p^64d^05s^0$) as $\text{Y}_{0.8}^{3+}\text{Ca}_{0.2}^{2+}$ in the real material. Hartree potential is expanded in terms of lattice harmonics up to $L = 6$, and an exchange-correlation potential of von Barth-Hedin type [23] is taken within the local-(spin-) density approximation [L(S)DA]. $8 \times 8 \times 2$ ($k_x \times k_y \times k_z$), $8 \times 8 \times 1$, and $6 \times 6 \times 2$ special \mathbf{k} points in $1/8$ irreducible Brillouin zone are respectively used for the self-consistent calculations of $\text{Sr}_2\text{CoO}_3\text{Cl}$, $\text{Sr}_3\text{Co}_2\text{O}_5\text{Cl}_2$, and $\text{Sr}_2\text{Y}_{0.8}\text{Ca}_{0.2}\text{Co}_2\text{O}_6$. A small number

of the \mathbf{k} points are taken along the c axis due to the large c -axis constant and to the two-dimensional ab -planar structure.

Although L(S)DA can give some useful information for TMOs, its descriptions for TMOs are often unsatisfactory quantitatively and even erroneous qualitatively in some cases, *e.g.*, concerning the insulating ground state of FeO and CoO [24]. This is because TMOs are commonly classified as strongly correlated electron systems, whereas the L(S)DA in the framework of mean-field approximation underestimates the electron correlation effects. As such, the electron correlation should be included in a better way into electronic structure calculations of TMOs. Along this direction, on-site Coulomb correlation correction (so called LSDA+ U) method [24] proves rather powerful. For this reason, LSDA+ U calculations are performed with $U = 5 \text{ eV}$ for the Co $3d$ electrons [25]. As seen below, the present discussion is made mainly on the basis of the LSDA+ U results which are of more concern in this work.

3 Results

3.1 $\text{Sr}_2\text{CoO}_3\text{Cl}$

A spin-restricted LDA calculation is first performed for the paramagnetic (PM) state of $\text{Sr}_2\text{CoO}_3\text{Cl}$ in order to separate the crystal-field (CF) effect from the magnetic exchange splitting. It can be seen in Figure 1a that the Co $3d$ bands lie between -1 and 2 eV relative to E_F , the ab -planar O $2p$ bands range approximately from -7.5 to -2 eV , the apical c -O $2p$ bands are relatively narrow and located between -5.5 to -2 eV , and the apical Cl $3p$ bands are a little lower than the c -O $2p$ ones. In contrast, the very narrow Sr $4p$, O $2s$, and Cl $3s$ bands lie at deep levels of -15 , -18 eV , and that between them, respectively; whereas the empty Sr $4d5s$ bands lie above 5 eV and the Co $4s$ one even higher. Both the deep and high-level bands have a negligible contribution to the most concerned pd valence bands ranging from -8 to 2 eV , and therefore they are not shown here. In the RT tetragonal structure, the Co $3d$ xz/yz doublet has the lowest level, which is followed by a little higher xy singlet. The $x^2 - y^2$ level is highest and the $3z^2 - r^2$ one is second highest. The narrow xz/yz and xy bands have weak $pd\pi$ hybridizations with the neighboring O $2p$ orbitals, as is indicated by their small component in the lower-level bonding states. While the $x^2 - y^2$ and $3z^2 - r^2$ bands have a large bonding-antibonding splitting due to strong $pd\sigma$ hybridizations, and a pronounced bonding state between the $x^2 - y^2$ and the ab -O $p_{x,y}$ orbitals appears at -5.5 eV , and that between the $3z^2 - r^2$ and c -O p_z orbitals at -4.5 eV . Whereas the Co $3d$ orbitals almost have no interaction with the Cl $3p$ one due to a long Co-Cl distance of 3.116 \AA , as is indicated by no corresponding bonding and antibonding states. In a sense, the CoO_5Cl octahedron in $\text{Sr}_2\text{CoO}_3\text{Cl}$ can be viewed as a CoO_5 pyramid. In addition, a point-charge model calculation for the given structure of the $\text{Co}^{3+}\text{O}_5^{2-}\text{Cl}^-$ octahedron shows that the Co $3d$ CF levels

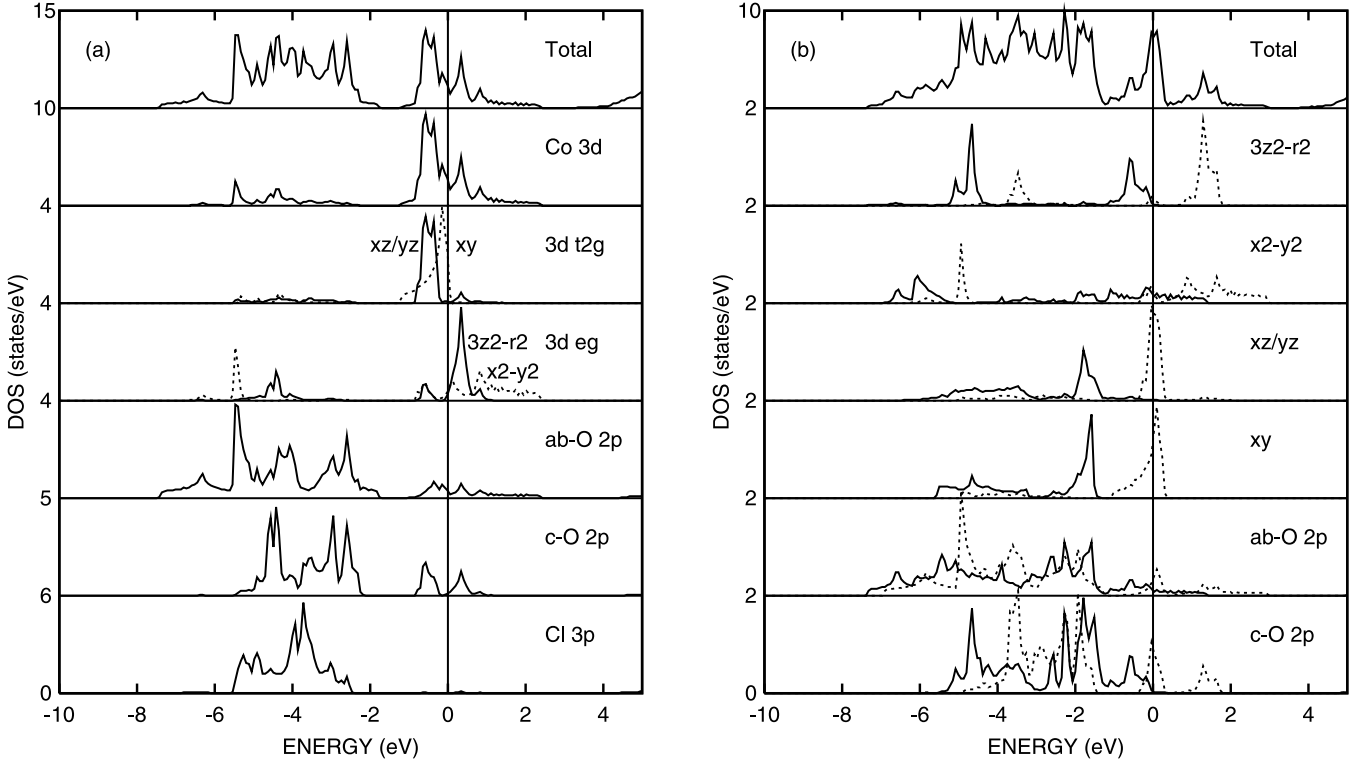


Fig. 1. The (a) LDA-PM and (b) LSDA-FM DOS of $\text{Sr}_2\text{CoO}_3\text{Cl}$. Fermi level is set at zero. For the orbital-resolved DOS in (b), the solid (dashed) line denotes the majority (minority) spin channel. See discussions in main text.

are ordered in units of eV as $(xz/yz, 0, \text{reference zero energy})$, $(3z^2 - r^2, 0.11)$, $(xy, 0.23)$, and $(x^2 - y^2, 0.51)$. A reverse of the $3z^2 - r^2$ and xy levels in the above band data is attributed to the modified Coulomb potential arising from a real charge distribution other than the idealized point charge. It is evident that the Co^{3+} ion sees a reduced CF in $\text{Sr}_2\text{CoO}_3\text{Cl}$ due to a strong deformation of the CoO_5 pyramid, especially a strong plane corrugation $D = 0.325 \text{ \AA}$. As a result, the Co^{3+} ion strongly tends to take a high-spin (HS) ground state to lower exchange energy by Hund coupling [17].

For the above reason, a spin-polarized LSDA calculation is performed below for the assumed ferromagnetic (FM) state. The Co 3d and O 2p bands undergo significant changes due to strong magnetic exchange interactions. The majority-spin t_{2g} (xz/yz and xy) and the $3z^2 - r^2$ orbitals become filled up, and the majority-spin $x^2 - y^2$ orbital couples to the ab -O $p_{x,y}$ ones and hence forms conduction bands wider than 3 eV, as seen in Figure 1b. The minority-spin e_g ($3z^2 - r^2$ and $x^2 - y^2$) orbitals are nearly empty, while the minority-spin t_{2g} bands, being nearly degenerate and very narrow, just lie at E_F and thus give a high DOS (density of states) peak at E_F . This DOS peak implies an instability of the RT tetragonal structure. The calculated Co^{3+} spin moment is $2.5 \mu_B$, and the pd hybridizations induce a non-negligible spin moment of 0.15 (0.31) μ_B at the ab -O (c -O) site. The ab -O spin is smaller than the c -O one due to a delocalization of the ab -O $p_{x,y}$ electrons. Whereas the Sr^{2+} and Cl^- ions have a very

minor moment of only about $0.01 \mu_B$. Note that either the Co^{3+} spin alone or the total spin of $3.1 \mu_B$ per formula unit (fu) is larger than a spin-only value of $2 \mu_B$ for an intermediate-spin (IS, $t_{2g}^5 e_g^1$, $S = 1$) state which turns out to be unstable and converges to the present spin-polarized state. Moreover, the total energy of this state is lower than that of the above low-spin (LS, $t_{2g}^6 e_g^0$, $S = 0$) PM state by 0.02 eV/fu , which is significantly increased up to 0.10 eV/fu in the LSDA+ U calculations. These results suggest that the Co^{3+} ion takes a HS ($t_{2g}^4 e_g^2$, $S = 2$) ground state in $\text{Sr}_2\text{CoO}_3\text{Cl}$ [26], as is further supported by the following LSDA+ U calculations.

It can be seen in Figure 2 that the electron correlations significantly enhance the Co orbital- and spin-polarization. The Co 3d orbitals become strongly localized, and the majority-spin 3d orbitals are completely occupied except for the nearly filled-up $x^2 - y^2$ one [27]. The ab -planar O 2p orbitals coupled to this $x^2 - y^2$ one contribute to only $0.07 pd\sigma$ holes per CoO_2 basal square in the FM state as seen in Figure 2a. The Co spin moment (total one per formula unit) is increased up to 3.15 (3.8) μ_B , both of which are close to the HS state. It is evident that the upper valence bands (lower conduction bands) arise from the ab -O 2p states (the Co 3d ones), thus leading to a classification of $\text{Sr}_2\text{CoO}_3\text{Cl}$ as a p - d charge-transfer (CT) oxide [28] like an ordinary late 3d TMO. The formation of the above $pd\sigma$ holes having mainly the ab -O 2p character is closely related to such a p - d CT nature. Although

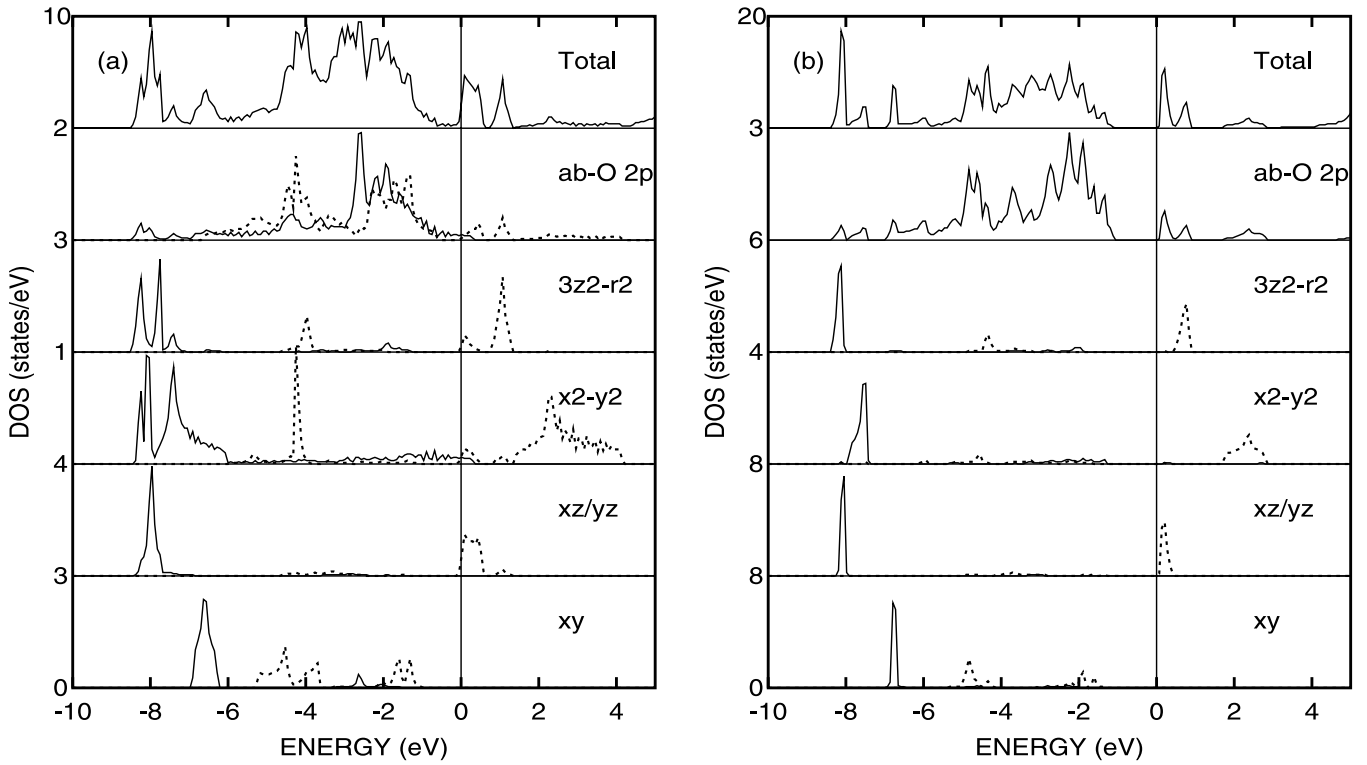


Fig. 2. The LSDA+ U DOS for the (a) FM and (b) AFM states of $\text{Sr}_2\text{CoO}_3\text{Cl}$. (a) It is evident that the Co^{3+} ion takes a HS state and only 0.07 ab -planar $pd\sigma$ holes per CoO_2 basal square have mainly the ab -O $2p$ character in this CT-type TMO. (b) The HS-coupled AFM insulating ground state is stabilized by opening a CT gap of 1.28 eV.

delocalized $pd\sigma$ holes tend to induce a FM metallicity conceptually *via* the p - d exchange [21] due to the dominant O $2p$ hole character (rather than the double-exchange [29]), the small amount of (only 0.07) holes are insufficient to induce an actual FM metallic state for $\text{Sr}_2\text{CoO}_3\text{Cl}$. Instead a strong superexchange (SE) AFM coupling exists between the HS Co^{3+} ions [20], and the dominant AFM coupling strongly suppresses the bandwidths and naturally yields an insulating ground state with a large CT gap of 1.28 eV (see Fig. 2b) which has lower total energy than the above FM state by 0.48 eV/fu. The calculated spin moment of the HS Co^{3+} ion is reduced to $3.17 \mu_B$ in this AFM state due to finite pd hybridizations. Thus, the in-plane nearest-neighbor exchange integral is estimated to be $J_{ab} \approx 48$ meV, if the Heisenberg model applies.

3.2 $\text{Sr}_3\text{Co}_2\text{O}_5\text{Cl}_2$

Since LSDA+ U calculations are more concerned in this work as stated in Section 2, here only the LSDA+ U results are shown.

In the FM state (see Fig. 3), the majority-spin Co^{3+} t_{2g} and $3z^2 - r^2$ orbitals are completely occupied, and the majority-spin $x^2 - y^2$ orbital is nearly full-filled. While the little more half-filled minority-spin xz/yz doublet, by

allowing orbital polarization, splits and forms an xz/yz orbital ordered (OO) state which is to be stabilized by a cooperative Jahn-Teller (JT) distortion as discussed below. In this CT-type LCO, the ab -planar O $2p$ orbitals couple to the $x^2 - y^2$ one and form wide conduction bands. In particular, the majority-spin $pd\sigma$ band contributes to 0.22 delocalized holes per CoO_2 basal square. The increasing amount of $pd\sigma$ holes from 0.07 in 1L $\text{Sr}_2\text{CoO}_3\text{Cl}$ to 0.22 in 2L $\text{Sr}_3\text{Co}_2\text{O}_5\text{Cl}_2$ suggest a stronger electron delocalization in the latter. Correspondingly, the calculated Co $3d$ (ab -O $2p$) spin moment decreases from 3.15 ($0.17 \mu_B$) in $\text{Sr}_2\text{CoO}_3\text{Cl}$ to 3.10 ($0.14 \mu_B$) in $\text{Sr}_3\text{Co}_2\text{O}_5\text{Cl}_2$ as seen in Table 1. As seen in reference [5], $\text{Sr}_2\text{CoO}_3\text{Cl}$ and $\text{Sr}_3\text{Co}_2\text{O}_5\text{Cl}_2$ have an almost identical ab -planar Co-O bond-length with a difference only 0.001 Å. Naturally the enhanced electron delocalization in the latter can be ascribed to the decreasing D from 0.325 Å in the former to 0.285 Å in the latter, which corresponds to an increasing ab -planar Co-O-Co bond angle from 161.1 to 163.6 degree [5].

The Co^{3+} ion takes an almost HS state in the assumed FM state of $\text{Sr}_3\text{Co}_2\text{O}_5\text{Cl}_2$ as shown above [26]. The 0.22 delocalized $pd\sigma$ holes could yield a FM metallic-like signal *via* the p - d exchange coupling [21]. Here it is recalled that in the layered-type double perovskite $\text{TbBaCo}_2\text{O}_{5.5}$ with a decreasing D ($D = 0.19$ and 0.32 Å in the deformed CoO_6 octahedron and CoO_5 pyramid in the 270-K phase,

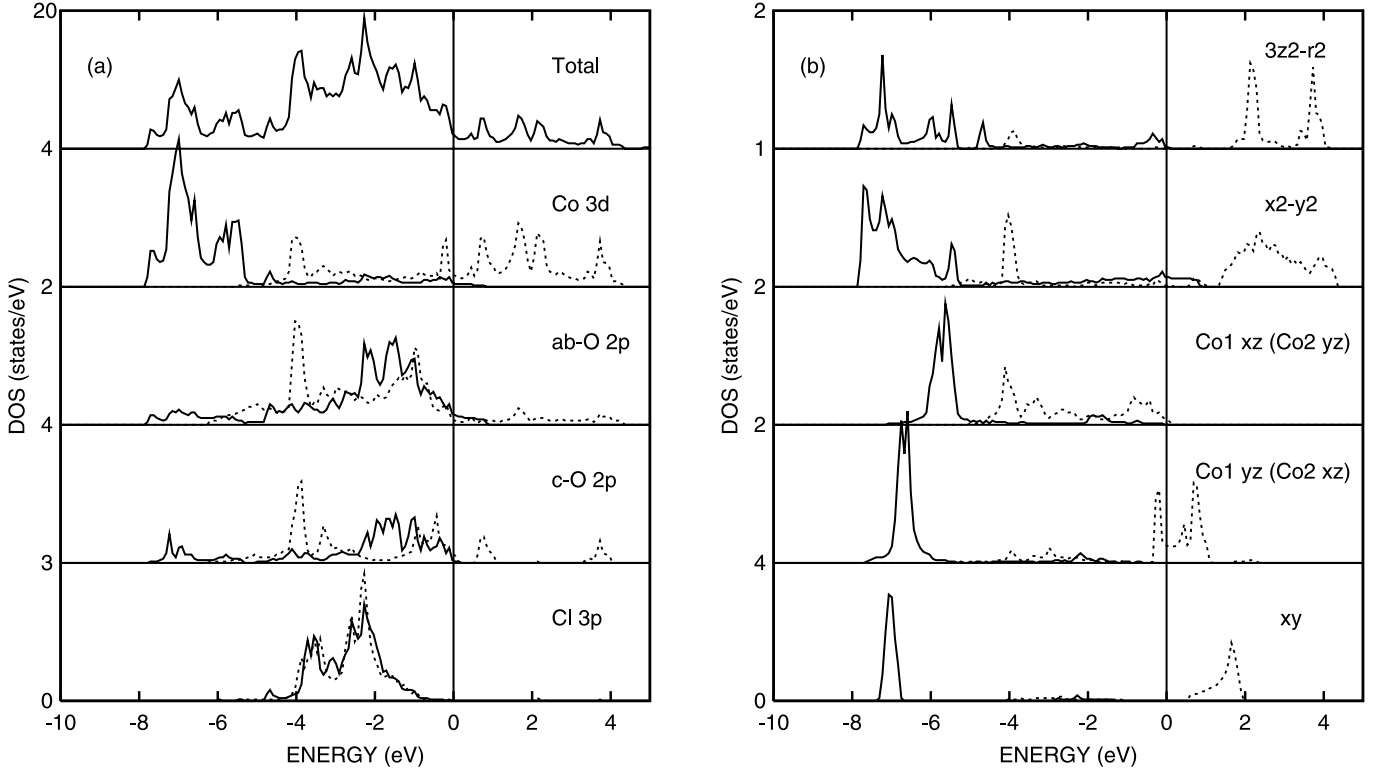


Fig. 3. The LSDA+ U DOS for the FM state of $\text{Sr}_3\text{Co}_2\text{O}_5\text{Cl}_2$. The solid (dashed) line denotes the majority (minority) spin. The Co^{3+} ion takes an almost HS state, and there are 0.22 *ab*-planar *pd* σ holes per CoO_2 basal square. This FM state, with an *xz/yz* OO to be stabilized by a JT lattice distortion, is expected to evolve into a HS-AFM insulating ground state as shown in Figure 2.

Table 1. Electron occupation number/spin moment (in μ_B) calculated by LSDA+ U ($U = 5$ eV) for the FM and/or AFM states.

	$\text{Sr}_2\text{CoO}_3\text{Cl}$		$\text{Sr}_3\text{Co}_2\text{O}_5\text{Cl}_2$	$\text{Sr}_2\text{Y}_{0.8}\text{Ca}_{0.2}\text{Co}_2\text{O}_6$
	FM	AFM	FM	FM
Co 3d	7.13/3.15	7.12/3.17	7.09/3.10	7.02/3.06
<i>a</i> -O 2p	5.32/0.17	5.30/0	5.30/0.14	5.43/0.04
<i>b</i> -O 2p	5.32/0.17	5.30/0	5.30/0.14	5.56/0.04
<i>c</i> -O 2p	5.24/0.32	5.23/0	5.19/0.26	5.32/0.15
<i>c</i> -Cl 3p	5.73/0.03	5.72/0	5.75/0.02	

respectively) [16], the delocalized *pd* σ holes within the *ab*-plane are remarkably increased up to 0.61 per formula unit and they contain 0.305 per CoO_2 basal square on average [18]. Moreover, there are 0.24 holes which are delocalized along the *c*-axis CoO chain formed by the apex-shared CoO_6 octahedra [18]. As discussed in reference [18], the increasing amount of holes in the almost HS state of $\text{TbBaCo}_2\text{O}_{5.5}$ are responsible for an appearance of a FM state at 260–340 K with a sudden drop of resistivity, and for a high- T PM metallic state. Whereas the strong HS-coupled AFM insulating behavior is inherent and competes with the FM metallicity, thus leading to FM-AFM and metal-insulator (M-I) transitions in $\text{TbBaCo}_2\text{O}_{5.5}$. In

the sense, a HS AFM insulating ground state is also expected for 2L $\text{Sr}_3\text{Co}_2\text{O}_5\text{Cl}_2$, although a finite FM signal could appear due to the hole delocalization with increasing T . However, no real calculation is attempted here for the AFM state of $\text{Sr}_3\text{Co}_2\text{O}_5\text{Cl}_2$ because of a high computational cost for the large unit cell.

3.3 $\text{Sr}_2\text{Y}_{0.8}\text{Ca}_{0.2}\text{Co}_2\text{O}_6$

LSDA+ U calculation for the assumed FM state of $\text{Sr}_2\text{Y}_{0.8}\text{Ca}_{0.2}\text{Co}_2\text{O}_6$ shows that the majority-spin t_{2g} and

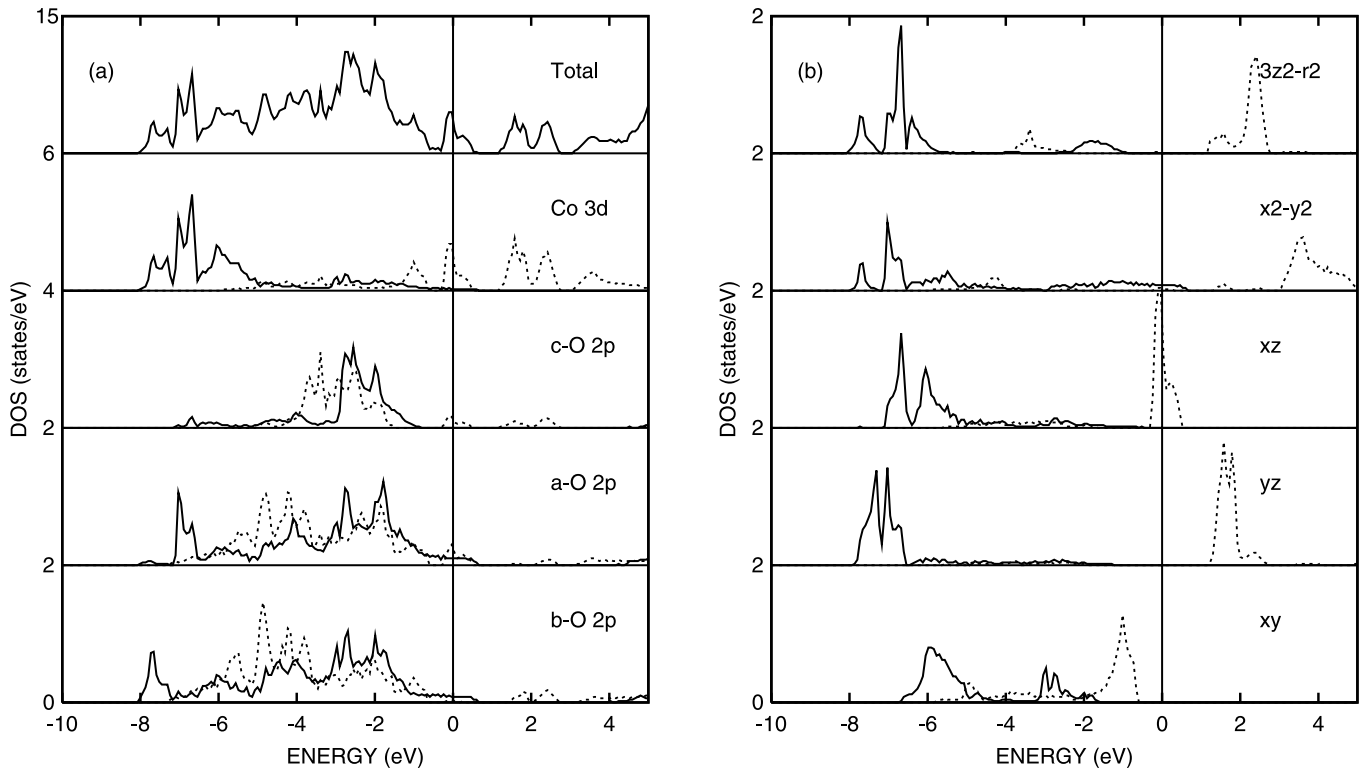


Fig. 4. The LSDA+ U DOS for the FM state of $\text{Sr}_2\text{Y}_{0.8}\text{Ca}_{0.2}\text{Co}_2\text{O}_6$. The $\text{Co}^{2.6+}$ ion take a HS state, and the 0.13 ab -planar $pd\sigma$ holes per CoO_2 basal square are mainly due to the rising $\text{Co}^{2.6+}$ $3d$ levels (for comparison see the Co^{3+} $3d$ levels in Fig. 2a).

$3z^2 - r^2$ orbitals and the minority-spin xy orbital are completely occupied (see Fig. 4). The majority-spin $x^2 - y^2$ orbital couples to the a - and b -axis O $2p$ ones and contributes to 0.13 $pd\sigma$ holes per CoO_2 square, while the minority-spin xz narrow band is partly occupied and just lies at E_F . As indicated by experiments [7], $D = 0.44 \text{ \AA}$ in $\text{Sr}_2\text{Y}_{0.8}\text{Ca}_{0.2}\text{Co}_2\text{O}_6$ is much larger than $D = 0.325 \text{ \AA}$ in $\text{Sr}_2\text{CoO}_3\text{Cl}$ [5]. A weaker $pd\sigma$ hybridization and thus a stronger electron localization, and therefore a stronger ionicity should occur in the former, as is supported by the present results (i–iv) as seen in Table 1. (i) The formal $\text{Co}^{2.6+}$ (Co^{3+}) ion takes the $3d^{6.4}$ ($3d^6$) state in $\text{Sr}_2\text{Y}_{0.8}\text{Ca}_{0.2}\text{Co}_2\text{O}_6$ ($\text{Sr}_2\text{CoO}_3\text{Cl}$), while the calculated occupation number of the $\text{Co}^{2.6+}$ $3d$ orbital is about 0.1 smaller than that of the Co^{3+} one. (ii) The calculated Co spin moment of $3.06 \mu_B$ attains 85% spin polarization of the HS $\text{Co}^{2.6+}$ ($3.6 \mu_B$) ion, while the corresponding spin polarization is weaker than 80% in both $\text{Sr}_2\text{CoO}_3\text{Cl}$ and $\text{Sr}_3\text{Co}_2\text{O}_5\text{Cl}_2$. (iii) The ab -O and c -O ionic charge increases by 0.1–0.25 and 0.1, respectively. (iv) Reduced pd hybridizations induce a smaller oxygen spin moment, $0.04 \mu_B$ for the a - and b -axis oxygens, and $0.15 \mu_B$ for the c -axis oxygen. Owing to only a minor difference (smaller than 0.03 \AA) [5,7] between the ab -planar Co-O bond length of $\text{Sr}_2\text{Y}_{0.8}\text{Ca}_{0.2}\text{Co}_2\text{O}_6$ and that of $\text{Sr}_2\text{CoO}_3\text{Cl}$, instead the variance of the D parameter, and the corresponding variance of the planar Co-O-Co bond angle from 161.1 degree in $\text{Sr}_2\text{CoO}_3\text{Cl}$ [5] to $151.2/157.2$ degree in

$\text{Sr}_2\text{Y}_{0.8}\text{Ca}_{0.2}\text{Co}_2\text{O}_6$ [7] are believed to play a leading role in their electronic-structure variances. Speaking qualitatively, increasing D would lead to a decreasing amount of planar delocalized $pd\sigma$ holes in LCOs. Note that effective charge of different Co valent state in LCOs affects the level distributions also. It is therefore not surprising that the $pd\sigma$ hole number is larger in $\text{Sr}_2\text{Y}_{0.8}\text{Ca}_{0.2}\text{Co}_2\text{O}_6$ than in $\text{Sr}_2\text{CoO}_3\text{Cl}$, because the $\text{Co}^{2.6+}$ $3d$ levels of the former, lying higher than the Co^{3+} ones of the latter, couple to the ab -O $2p$ states and contribute to a little more holes. However, these holes are more localized in $\text{Sr}_2\text{Y}_{0.8}\text{Ca}_{0.2}\text{Co}_2\text{O}_6$ than in $\text{Sr}_2\text{CoO}_3\text{Cl}$ as shown above.

Owing to the large D and strong hole localization in $\text{Sr}_2\text{Y}_{0.8}\text{Ca}_{0.2}\text{Co}_2\text{O}_6$, this LCO is expected to be a HS AFM insulator like layered $\text{LnBaCo}_2\text{O}_5$ ($\text{Ln} = \text{Y, Tb, Dy, Ho}$) with $D \sim 0.4 \text{ \AA}$ at RT [14,15,17], although no real calculation is performed for the AFM state with a large unit cell.

4 Discussion

The RT tetragonal structure of both $\text{Sr}_2\text{CoO}_3\text{Cl}$ and $\text{Sr}_3\text{Co}_2\text{O}_5\text{Cl}_2$ seems unstable because of the $\text{Co}^{3+} t_{2g}$ -level near degeneracy and/or the half-filled xz/yz doublet, as indicated in the above calculations. This is also the case for the layered $\text{LnBaCo}_2\text{O}_5$ ($\text{Ln} = \text{Y, Tb, Dy, Ho}$) (see Fig. 2 in Ref. [17]). As observed experimentally [14,15],

$\text{LnBaCo}_2\text{O}_5$ actually undergo a $\text{Co}^{2+}/\text{Co}^{3+}$ charge-ordering (CO) transition and transform from the RT $Pm\bar{m}m$ structure to the low- T $Pmma$ one. A corresponding JT lattice distortion occurs in $\text{LnBaCo}_2\text{O}_5$ and the resulting difference between the a - and b -axis Co-O bond lengths is about 0.05–0.1 Å [15]. As a result, the near degeneracy of the t_{2g} states is lifted in $\text{LnBaCo}_2\text{O}_5$, and the minority-spin xz/yz and xy orbitals are occupied out of the t_{2g} ones for the HS Co^{2+} and Co^{3+} ions, respectively [17]. Correspondingly, $\text{Sr}_2\text{CoO}_3\text{Cl}$ and $\text{Sr}_3\text{Co}_2\text{O}_5\text{Cl}_2$ are expected to transit into a low- T distorted phase (likely orthorhombic) with alternate ab -planar Co-O bond-lengths. A difference between these bond-lengths, about 0.05–0.1 Å typical of a weak JT distortion seen by the t_{2g} electrons, is believed to be large enough to lift the (near) degeneracy of the t_{2g} orbitals and to strongly split the xz/yz doublet with the aid of the $3d$ electron correlations [18], thus giving rise to an xz/yz OO insulating ground state for $\text{Sr}_2\text{CoO}_3\text{Cl}$ and $\text{Sr}_3\text{Co}_2\text{O}_5\text{Cl}_2$. If this OO state were a true ground state, a superlattice diffraction would be observed. Moreover, it is believed that the reduced CF itself undergoes only a slight change in the OO state (as in the CO state of $\text{LnBaCo}_2\text{O}_5$ [17]) and does not modify the above (almost) HS state or affect the present discussion.

One could also expect a presence of a finite Co orbital moment and a spin-orbital coupling (SOC) in $\text{Sr}_2\text{CoO}_3\text{Cl}$ and $\text{Sr}_3\text{Co}_2\text{O}_5\text{Cl}_2$, since the localized Co $3d$ electrons see a reduced CF. However, the SOC commonly has an order of magnitude of only 0.01 eV in the $3d$ TMOs, and it is significantly weaker than the Hund coupling typical of ~ 1 eV. Therefore, a negligence of the weak SOC effect in the present calculations does not at least affect the present conclusion concerning the Co^{3+} (almost) HS state. But note that since the t_{2g} orbitals are near degenerate in the RT tetragonal structure, the SOC could be operative by lowering the $L_z = \pm 1$ ($xz \pm iyz$) singlets at the alternate AFM-coupled Co sites, thus inducing alternate orbital moments of $\pm 1 \mu_B$. Thus either this state or the above OO state calls for a further study.

It is evident that the lately synthesized LCOs belong to two-dimensional systems from the viewpoints of both their crystallographical and electronic structures, and the plane corrugation of the CoO_2 basal layer is a common structure feature of them, which leads to a reduced CF seen by the Co ions. In the cobalt-trivalent SCOC series (1L $\text{Sr}_2\text{CoO}_3\text{Cl}$, 2L $\text{Sr}_3\text{Co}_2\text{O}_5\text{Cl}_2$ and 3L $\text{Sr}_4\text{Co}_3\text{O}_{7.5}\text{Cl}_2$), the ab -planar Co-O bond-lengths vary very slightly around 1.97 Å within a range of 0.01 Å [5]. While it was also found [5] that D decreases monotonously ($D_{1L} = 0.325 \text{ Å} > D_{2L} = 0.285 \text{ Å} > D_{3L} = 0.266 \text{ Å}$) in the SCOC series with the increasing number of the layers (due to a covalence contraction caused by an interlayer coupling). It is therefore firmly believed that the varying D (and thus varying planar Co-O-Co bond-angles) is essentially responsible for the evolutions of electronic, magnetic, and transport properties of the SCOC series. The decrease of D in the SCOC series, as shown in the above calculations, leads to the rising $x^2 - y^2$ level and

enhanced planar $pd\sigma$ hybridizations and electron delocalization, and hence to an increasing amount of delocalized $pd\sigma$ holes in the almost HS state. The delocalized $pd\sigma$ holes have mainly the ab -O $2p$ character in these CT-type SCOC. The mobile O $2p$ holes are antiferromagnetically coupled to the Co $3d$ spins, and hence they tend to induce an effective FM coupling (between the Co spins) and a metallic-like behavior *via* the p - d exchange rather than the double-exchange. However, the delocalized holes seem insufficient to induce an actual FM metallic state in SCOC, compared with the case of the AFM-FM and I-M transition material $\text{TbBaCo}_2\text{O}_{5.5}$ with smaller D and more holes, as stated in Section 3.2. As indicated above, $\text{Sr}_2\text{CoO}_3\text{Cl}$ takes a HS AFM insulating ground state, and so is expected for $\text{Sr}_3\text{Co}_2\text{O}_5\text{Cl}_2$, and $\text{Sr}_4\text{Co}_3\text{O}_{7.5}\text{Cl}_2$ as well although no real calculation is performed for it due to a random distribution of the 0.5 oxygen holes. While the increasing amount of $pd\sigma$ holes consistently account for the decreasing resistivities and effective magnetic moments (μ_{eff}) as observed in SCOC [5] with the increasing number of the layers. Since D is larger in SCOC than in the layered-type $\text{TbBaCo}_2\text{O}_{5.5}$ but smaller than in $\text{LnBaCo}_2\text{O}_5$ as shown above, the electronic, magnetic, and transport properties of the SCOC series can be qualitatively understood as an intermediate phase between the AFM-FM and I-M transition material $\text{TbBaCo}_2\text{O}_{5.5}$ and the complete HS coupled SE-AFM insulator $\text{LnBaCo}_2\text{O}_5$.

The measured insulating behavior of the SCOC series [5] can be explained here. Whereas the original suggestion [5] of their magnetic properties differs much from the present results in that no magnetic ordering was detected and a small Co^{3+} $\mu_{eff} = 0.80$ (0.56) μ_B was extracted in the so-called LS $\text{Sr}_2\text{CoO}_3\text{Cl}$ ($\text{Sr}_3\text{Co}_2\text{O}_5\text{Cl}_2$). It seems that the original suggestion was only based on a fitting of the inverse magnetic susceptibility (χ^{-1}) data measured below 250 K to a simple Curie-Weiss law [5]. It is argued that such a measurement and a fitting are insufficient, since the AFM interaction temperature in SCOC (*e.g.*, $J_{ab} \approx 48$ meV in $\text{Sr}_2\text{CoO}_3\text{Cl}$) is expected to be near RT (probably between the $T_N = 260$ K of $\text{TbBaCo}_2\text{O}_{5.5}$ [16] and 330–340 K of $\text{LnBaCo}_2\text{O}_5$ [14,15]). Therefore, further experiments such as a measurement of χ above RT and neutron diffraction would provide more informative magnetism data. Moreover, it is worth noting that the present conclusion on the HS state of $\text{Sr}_2\text{CoO}_3\text{Cl}$ is supported by a late joint study [30] of O- K and Co- $L_{2,3}$ X-ray absorption spectra (XAS) and charge-transfer multiplet calculations.

Now we turn to the 2L $\text{Sr}_2\text{Y}_{1-x}\text{Ca}_x\text{Co}_2\text{O}_{6+\delta}$. The structure of $\text{Sr}_2\text{Y}_{0.8}\text{Ca}_{0.2}\text{Co}_2\text{O}_6$ [7] can be viewed as a $\text{SrY}_{0.8}\text{Ca}_{0.2}\text{Co}_2\text{O}_5$ bilayer plus a SrO monolayer. The $\text{SrY}_{0.8}\text{Ca}_{0.2}\text{Co}_2\text{O}_5$ bilayer containing the apical-oxygen deficient CoO_5 pyramids shares a great similarity to the structure of $\text{LnBaCo}_2\text{O}_5$ ($\text{Ln} = \text{Y, Tb, Dy, Ho}$; $D \sim 0.4 \text{ Å}$ at RT) which are also of current interest [14,15]. The 0.13 holes per CoO_2 square in the assumed FM state of $\text{Sr}_2\text{Y}_{0.8}\text{Ca}_{0.2}\text{Co}_2\text{O}_6$ are mainly due to the rising $\text{Co}^{2.6+}$ $3d$ levels (compared with the Co^{3+} case in above SCOC) and the corresponding $pd\sigma$ hybridizations. While these holes are more localized than those in SCOC,

because a larger D ($=0.44 \text{ \AA}$ in the 260 K structure [7]) in $\text{Sr}_2\text{Y}_{0.8}\text{Ca}_{0.2}\text{Co}_2\text{O}_6$ strongly reduces the *ab*-planar *pd* σ hybridizations. The present calculated Co spin moment of $3.06 \mu_B$ is close to an experimental value of $2.93 \mu_B$ [7] and attains 85% spin polarization of the ideal $3.6 \mu_B$ for the formal HS $\text{Co}^{2.6+}$ ion, and it is also close to the previously calculated $3.1 \mu_B$ for the HS $\text{Co}^{2.5+}$ ($3.5 \mu_B$) ion in the AFM *Pmmm* structure of YBaCo_2O_5 [17]. It is therefore not surprising that the HS $\text{Sr}_2\text{Y}_{0.8}\text{Ca}_{0.2}\text{Co}_2\text{O}_6$ ($\text{Sr}_2\text{Y}_{1-x}\text{Ca}_x\text{Co}_2^{2.5+}\text{O}_{6-\delta}$) is an AFM insulator [6,7] with a high $T_N \approx 270 \text{ K}$ (300 K) like $\text{LnBaCo}_2\text{O}_5$ [14,15]. While both the formal non-integer $\text{Co}^{2.6+}$ valence and a partial filling of the minority-spin *xz* narrow band (but a complete filling of the lower-level *xy* band due to the large D) imply an instability of $\text{Sr}_2\text{Y}_{0.8}\text{Ca}_{0.2}\text{Co}_2\text{O}_6$ against a structure distortion, which could induce a superstructure and form a charge disproportion and/or OO at low- T . Thus the holes become more strongly localized.

For $\text{Sr}_2\text{Y}_{1-x}\text{Ca}_x\text{Co}_2\text{O}_{6+\delta}$, it can be assumed that the apical-oxygen holes of the CoO_5 pyramids are gradually removed as δ increases, and instead more CoO_6 octahedra appear and thus D decreases as clearly seen in $\text{TbBaCo}_2\text{O}_{5+\delta}$ ($\delta = 0$, $D \sim 0.4 \text{ \AA}$; $\delta = 0.5$, averaged $D \sim 0.25 \text{ \AA}$) [15,16]. Thus it is naturally expected, according to the above calculations and discussion, that as δ increases (D decreases) the Co ion evolves from a complete HS state to an almost HS state with an increasing amount of delocalized *pd* σ holes. Note that this expectation is also supported by the late O-*K* and Co- $L_{2,3}$ XAS study [30] for $\text{Sr}_2\text{Y}_{0.5}\text{Ca}_{0.5}\text{Co}_2\text{O}_{6+\delta}$ ($\delta = -0.248, 0.196, 0.645$). The increasing amount of delocalized holes tend to induce (*via* the *p-d* exchange) a FM metallic signal in large δ (and high cobalt valence) samples, which competes with the inherent HS-coupled SE-AFM insulating behavior. Thus a possible spin frustration gives rise to a spin-glassy insulating (semiconducting) state for the $\text{Co}^{3.4+}$ ($\text{Co}^{3.75+}$) sample with decreasing resistivity compared with the $\text{Co}^{2.6+}$ one $\text{Sr}_2\text{Y}_{0.8}\text{Ca}_{0.2}\text{Co}_2\text{O}_6$ [6,8].

As discussed above, the D parameter (and thus planar Co-O-Co bond angles) is essentially responsible for the physical properties of the lately synthesized LCOs, although their electronic structures are affected by both the effective charge of different cobalt valences and the planar Co-O bond lengths. The present LSDA+ U calculations indicate at least a tendency that as D decreases in the LCOs, the Co ion evolves from a HS state to an almost HS state with an increasing amount of the delocalized *pd* σ holes having mainly the planar O $2p$ character in these CT-type oxides. The former is responsible for an SE-coupled AFM insulating nature, while the latter gives rise to a coexistence of (and a competition between) the inherent AFM insulating behavior and the hole-mediated *p-d* exchange FM metallicity. It is a variance of the *pd* σ hole number that modifies the electronic, magnetic, and transport properties of the LCOs. Thus a general spin-state model and a qualitative physical picture have been proposed for the LCOs.

It was found in experiments that the SCOC series ($D \leq 0.266 \text{ \AA}$) are all insulating [5], and that

$\text{TbBaCo}_2\text{O}_{5.5}$ (an averaged $D \sim 0.25 \text{ \AA}$) exhibits the AFM-FM and I-M transitions [16]. The LSDA+ U calculations show that $\text{Sr}_3\text{Co}_2\text{O}_5\text{Cl}_2$ and $\text{TbBaCo}_2\text{O}_{5.5}$ have 0.22 and 0.305 planar delocalized holes per CoO_2 basal square, respectively. A combination of both the experimental findings and the present results leads to a tentative suggestion that more than 0.3 delocalized holes per CoO_2 square are likely necessary for the I-M and/or AFM-FM transitions in LCOs, where D is probably smaller than 0.25 \AA . As such, the physical properties of LCOs can be modified by hole doping (D variance) through element substitutions, particularly through an ionic-size change of the neighboring layers on both sides of the cobalt-oxygen layer.

A large ionic-size difference between the apical O^{2-} and Cl^- ions (1.40 \AA *vs.* 1.81 \AA , six coordinated [31]) in the CoO_5Cl octahedron should be a structural origin for the plane corrugation in the above SCOC series. It can be postulated that F^- doping or substitution for the Cl^- , if operative, could make D smaller than 0.25 \AA , since the F^- radius [31] of 1.33 \AA is near the O^{2-} size. In this way, the I-M and/or AFM-FM transitions could occur in the F^- doped or substituted SCOC with increasing hole number. In particular, a cobalt analog of the fascinating layered manganite $(\text{La,Sr})_{n+1}\text{Mn}_n\text{O}_{3n+1}$ [32] could emerge with FM metallic layers. Apart from the parent insulator SCOC, a few likely intriguing properties of the F^- doped or substituted SCOC, like CMR of $\text{La}_{2-2x}\text{Sr}_{1+2x}\text{Mn}_2\text{O}_7$ [32] or superconductivity of the layered $\text{Sr}_2\text{CuO}_2\text{F}_{2+\delta}$ [33] may deserve experimental investigations.

Moreover, the present picture could be employed for the 2L $\text{Bi}_2\text{A}_3\text{Co}_2\text{O}_{8+\delta}$ ($A = \text{Ca, Sr, Ba}$). It can be reasonably assumed that with increasing A size, the planar oxygens move towards the apical-oxygen-deficient A layer (see Fig. 1 in Ref. [9]) in a decreasing tendency, thus leading to a decreasing D . Thus the present picture could account for qualitatively the observed tendency [9] that $\text{Bi}_2\text{A}_3\text{Co}_2\text{O}_{8+\delta}$ varies from the semiconducting behavior for smaller $A = \text{Ca}$ and Sr (with larger D) to the semiconductor-metal transition for larger $A = \text{Ba}$ (with smaller D), as well as their increasing metallicity through lead doping (hole doping).

Furthermore, the present spin-state model may be an alternative even for the 1L $\text{La}_{2-x}\text{Sr}_x\text{CoO}_4$ containing an ideal CoO_2 plane ($D = 0$), for which an IS state model [12] and an ordered HS-LS model [13] were previously suggested separately. With increasing Sr doping (hole doping) in the well-defined HS AFM parent insulator La_2CoO_4 , the *ab*-planar Co-O bond-length decreases monotonously from 1.96 \AA ($x = 0$) to 1.91 \AA ($x = 1$) [12,34], which implies both an enhanced delocalization of the majority-spin *pd* σ hybridized $x^2 - y^2$ state and a gradual electron removal from (and thus hole injection into) the *pd* σ antibonding state. While the large *c*-axis Co-O bond-length, *e.g.*, for $x = 0$ and 1, varies slightly around 2.05 \AA [34], indicating that the localized majority-spin $3z^2 - r^2$ orbital remains filled up. As a result, the increasing amount of delocalized *pd* σ holes in the almost HS state, as in the above cases of SCOC, naturally account for the consistently

decreasing resistivity, μ_{eff} and Weiss temperature as observed [12] in $\text{La}_{2-x}\text{Sr}_x\text{CoO}_4$ upon Sr doping. Moreover, it was observed that their optical conductivity spectra ($E \parallel ab$) evolve from a single O $2p$ -Co $3d$ CT transition at ~ 3 eV for $x = 0.5$ to two CT transitions at ~ 2 eV and ~ 3 eV for $x = 1.0$ [35]. According to the present almost HS model, the additional structure at ~ 2 eV is ascribed to the transition from the ab -O $2p$ state to the delocalized majority-spin Co $3d x^2 - y^2$ hole state. If polarized ($E \parallel c$) spectra are to be measured, we suggest, the structure at ~ 2 eV will disappear according to the present model, whereas it will remain according to the ordered HS-LS model [13] where the $3z^2 - r^2$ hole state, besides the $x^2 - y^2$ one, is also available. To some extent such a measurement can check an applicability of the present model to $\text{La}_{2-x}\text{Sr}_x\text{CoO}_4$.

5 Conclusions

The lately synthesized LCOs—analogs of the superconducting layered cuprates and CMR layered manganites—exhibit rich and varying electronic, magnetic and transport properties [5–9]. They have a common structural feature—a plane corrugation (D) of the cobalt-oxygen layer, which gives rise to a reduced CF seen by the cobalt. As D decreases, the cobalt evolves from a HS to an almost HS with an increasing amount of the delocalized $pd\sigma$ holes having mainly the planar O $2p$ character in these CT-type LCOs, as well evidenced by the present LSDA+ U calculations and supported by a late O- K and Co- $L_{2,3}$ XAS study [30]. A competition between the HS-coupled SE-AFM insulating behavior and the delocalized-hole mediated FM metallicity (*via* the p - d exchange rather than the double-exchange) is responsible for a rich variety of phases of LCOs. The present picture, although seeming qualitative, is rather general for LCOs by a series of demonstrations. It is tentatively suggested that more than 0.3 delocalized holes per CoO_2 basal square are likely necessary for the I-M and/or AFM-FM transitions in LCOs with D probably smaller than 0.25 \AA . A phase control may be realized in LCOs by varying D (thus modifying the hole concentration) through an ionic-size change of the neighboring layers on both sides of the cobalt-oxygen layer, which leads to a search for likely novel LCOs. It could be also somewhat meaningful for other layered TMOs. Moreover, the present spin-state model may be applicable to those cobalt-based systems containing a basal-square-corrugated CoO_5 pyramid or CoO_6 octahedron. In addition, a few measurements of crystallography, magnetism, and spectroscopy are suggested for a check of the present model and picture.

The author is grateful to Z. Hu *et al.* [30] for communication of their results prior to publication and discussion with him, and thanks P. Fulde and A.-m. Hu for their suggestions. The author acknowledges Max-Planck Scholarship and hospitality of MPI-PKS.

References

1. M. Imada, A. Fujimori, Y. Tokura, Rev. Mod. Phys. **70**, 1039 (1998)
2. W.E. Pickett, D.J. Singh, Phys. Rev. B **53**, 1146 (1996), references therein
3. M.A. Senaris-Rodriguez, J.B. Goodenough, J. Solid State Chem. **118**, 323 (1995)
4. A. Maignan, C. Martin, D. Pelloquin, N. Nguyen, B. Raveau, J. Solid State Chem. **142**, 247 (1999)
5. S.M. Loureiro, C. Felser, Q. Huang, R.J. Cava, Chem. Mater. **12**, 3181 (2000)
6. K. Yamaura, Q. Huang, R.J. Cava, J. Solid State Chem. **146**, 277 (1999)
7. K. Yamaura, Q. Huang, R.W. Erwin, J.W. Lynn, R.J. Cava, Phys. Rev. B **60**, 9623 (1999)
8. K. Yamaura, D.P. Young, R.J. Cava, Phys. Rev. B **63**, 064401 (2001)
9. S.M. Loureiro, D.P. Young, R.J. Cava, R. Jin, Y. Liu, P. Bordet, Y. Qin, H. Zandbergen, M. Godinho, M. Nunez-Regueiro, B. Batlogg, Phys. Rev. B **63**, 094109 (2001)
10. R.H. Potze, G.A. Sawatzky, M. Abbate, Phys. Rev. B **51**, 11 501 (1995)
11. M.A. Korotin, S.Yu. Ezhov, I.V. Solovyev, V.I. Anisimov, D.I. Khomskii, G.A. Sawatzky, Phys. Rev. B **54**, 5309 (1996)
12. Y. Moritomo, K. Higashi, K. Matsuda, A. Nakamura, Phys. Rev. B **55**, R14 725 (1997)
13. J. Wang, W. Zhang, D.Y. Xing, Phys. Rev. B **62**, 14 140 (2000); J. Wang, Y.C. Tao, W. Zhang, D.Y. Xing, J. Phys. Cond. Matt. **12**, 7425 (2000)
14. T. Vogt, P.M. Woodward, P. Karen, B.A. Hunter, P. Henning, A.R. Moodenbaugh, Phys. Rev. Lett. **84**, 2969 (2000)
15. F. Fauth, E. Suard, V. Caignaert, B. Domenges, I. Mirebeau, L. Keller, Eur. Phys. J. B **21**, 163 (2001)
16. Y. Moritomo, T. Akimoto, M. Takeo, A. Machida, E. Nishibori, M. Takata, M. Sakata, K. Ohoyama, A. Nakamura, Phys. Rev. B **61**, R13 325 (2000)
17. H. Wu, Phys. Rev. B **62**, R11 953 (2000)
18. H. Wu, Phys. Rev. B **64**, 092413 (2001)
19. P. Hohenberg, W. Kohn, Phys. Rev. **136**, B864 (1964); W. Kohn, L.J. Sham, Phys. Rev. **140**, A1133 (1965)
20. P.W. Anderson, Phys. Rev. **115**, 2 (1959)
21. A.S. Alexandrov, A.M. Bratkovsky, Phys. Rev. Lett. **82**, 141 (1999); G.-M. Zhao, Phys. Rev. B **62**, 11 639 (2000)
22. H. Wu, M.C. Qian, Q.Q. Zheng, J. Phys. Cond. Matt. **11**, 209 (1999); H. Wu, Phys. Rev. B **64**, 125126 (2001)
23. U. von Barth, L. Hedin, J. Phys. C **5**, 1629 (1972)
24. V.I. Anisimov, J. Zaanen, O.K. Andersen, Phys. Rev. B **44**, 943 (1991); Pan Wei, Zheng Qing Qi, *ibid.* **49**, 10 864 (1994)
25. Parameter $U = 5$ eV is a reasonable choice for cobalt oxides both from its previous theoretical estimate [W.E. Pickett, S.C. Erwin, E.C. Ethridge, Phys. Rev. B **58**, 1201 (1998)] and its recent applications to YBaCo_2O_5 [17] and $\text{TbBaCo}_2\text{O}_{5.5}$ [18]. In addition, a varying $U = 4$ eV leads to only a minor decrease of the Co spin moment (the insulating gap), *e.g.*, by $0.07 \mu_B$ (0.14 eV) in $\text{Sr}_2\text{CoO}_3\text{Cl}$. The minor change does not affect the present discussion and conclusion made in the text

26. Strongly in contrast, the octahedrally coordinated Co ion in the pseudocubic perovskite LaCoO_3 sees a strong CF and takes a LS ground state [17], while a strong $pd\sigma$ hybridization stabilizes an IS state as the t_{2g} valence electrons are thermally excited to the broad e_g conduction bands with increasing temperature [11]. However, the pyramidally coordinated Co ion sees a weak CF in the LCOs and the Co $3d$ electrons have a decreasing $pd\sigma$ hybridization both due to the apical-oxygen deficiency and the strong base corrugation. The mechanism of forming the LS (IS) state by a strong CF (a strong $pd\sigma$ hybridization) seems ineffective in the LCOs, and therefore the HS state is preferable instead
27. There seems to be an uncertainty concerning the t_{2g} levels in $\text{Sr}_2\text{CoO}_3\text{Cl}$ due to their near degeneracy. Both the LDA calculation (Fig. 1a) and the point-charge model suggest that the xz/yz level is lower than the xy one as in $\text{Sr}_3\text{Co}_2\text{O}_5\text{Cl}_2$ (Fig. 3b). Whereas the minority-spin xy orbital has a little larger occupation number (*e.g.*, $n = 0.57$ in the LSDA-FM calculation) than the xz/yz doublet ($n = 0.51 \times 2$) because of a stronger pd hybridization for the former. Consequently, the xy level is lowered and becomes filled up (Fig. 2) by the U correction with the expression like $V_{m\sigma}^{\text{LSDA}+U} = V_{\sigma}^{\text{LSDA}} + (\frac{1}{2} - n_{m\sigma})U_{\text{eff}}$. This uncertainty is to be removed provided that the t_{2g} near degeneracy is lifted even by a weak Jahn-Teller distortion as discussed in the text
28. J. Zaanen, G.A. Sawatzky, J.W. Allen, Phys. Rev. Lett. **55**, 418 (1985)
29. C. Zener, Phys. Rev. **82**, 403 (1951)
30. Z. Hu, J. Baier, M. Haverkort, T. Lorenz, L.H. Tjeng, H.H. Hsieh, H.-J. Lin, C.T. Chen, C. Felser, (in preparation)
31. R.D. Shannon, Acta Cryst. **A32**, 751 (1976)
32. Y. Moritomo, A. Asamitsu, H. Kuwahara, Y. Tokura, Nature (London) **380**, 141 (1996)
33. M. Al-Mamouri, P.P. Edwards, C. Greaves, M. Slaski, Nature (London) **369**, 382 (1994)
34. T. Matsuura, J. Tabuchi, J. Mizusaki, S. Yamauchi, K. Fueki, J. Phys. Chem. Solids **49**, 1403 (1988)
35. S. Uchida, H. Eisaki, S. Tajima, Physica B **186-188**, 975 (1993); Y. Moritomo, T. Arima, Y. Tokura, J. Phys. Soc. Jpn **64**, L4117 (1995)